arXiv:cond-mat/0703222v1 [cond-mat.str-el] 8 Mar 2007

Anomalous thermal expansion and strong damping of the thermal conductivity of $NdMnO_3$ and $TbMnO_3$ due to $4f$ crystal-field excitations

K. Berggold, J. Baier, D. Meier, J.A. Mydosh, and T. Lorenz
II. Physikalisches Institut, Universität zu Köln, Zülpicher Str. 77, 50937 Köln, Germany

J. Hemberger
Experimentalphysik V, Institut für Physik, University of Augsburg, 86135 Augsburg, Germany

A. Balbashov
Moscow Power Engineering Institute, 105835 Moscow, Russia

N. Aliouane and D.N. Argyriou
Hahn-Meitner-Institut Berlin, Glienicker Str. 100, D-14109 Berlin, Germany

(Dated: February 6, 2008)

We present measurements of the thermal conductivity κ and the thermal expansion α of $NdMnO_3$ and $TbMnO_3$. In both compounds a splitting of the $4f$ multiplet of the R^{3+} ion causes Schottky contributions to α. In $TbMnO_3$ this contribution arises from a crystal-field splitting, while in $NdMnO_3$ it is due to the Nd–Mn exchange coupling. Another consequence of this coupling is a strongly enhanced canting of the Mn moments. The thermal conductivity is greatly suppressed in both compounds. The main scattering process at low temperatures is resonant scattering of phonons between different energy levels of the $4f$ multiplets, whereas the complex $3d$ magnetism of the Mn ions is of minor importance.

PACS numbers: 74.72.-h, 66.70.+f

I. INTRODUCTION

The search for magnetoelectric materials with the possibility to influence magnetic (electric) ordering by an electric (magnetic) field has greatly increased the interest in so-called multiferroic materials, in which magnetic and ferroelectric ordering phenomena coexist[1]. The orthorhombic rare-earth manganites RMnO$_3$ are particularly important here, since for $R =$ Gd, Tb, and Dy a ferroelectric phase develops within a magnetically ordered phase. These compounds show complex magnetic structures driven by frustration effects, and there is evidence that the ferroelectric order is related to a cycloidal magnetic ordering. Since the different magnetic and electric phase transitions strongly couple to lattice degrees of freedom[2,3,4], one may expect a strong influence of these ordering phenomena and the related low-lying excitations on the phonon thermal conductivity. In fact, recent zero-field thermal conductivity measurements of various RMnO$_3$ compounds by Zhou *et al.*[5] seem to support such a view. The thermal conductivity is found to be drastically suppressed for $R =$ Tb and Dy, while it shows a rather conventional behavior for the other RMnO$_3$ compounds. Thus, the authors of Ref. 5 interpreted the suppressed thermal conductivity of $R =$ Tb and Dy as a consequence of the complex ordering phenomena in these compounds. Based on the above conjecture we have studied the magnetic-field influence on the thermal conductivity of multiferroic $TbMnO_3$ and of $NdMnO_3$ which shows a more conventional antiferromagnetic order. A detailed analysis of the thermal conductivity in combination with results from thermal expansion measurements of $NdMnO_3$ and $TbMnO_3$ reveals that for both compounds the suppression of the thermal conductivity is largely determined by resonant scattering of phonons by different energy levels of the $4f$ orbitals. Therefore, our new results are in strong contrast to the interpretation proposed in Ref. 5.

The starting compound of the RMnO$_3$ series, $LaMnO_3$, crystallizes in an orthorhombic crystal structure (Pbnm) with a $GdFeO_3$ type distortion. If La is replaced by smaller rare-earth ions the $GdFeO_3$ type distortion increases, which causes a decreasing Mn-O-Mn bond angle. In $LaMnO_3$, a Jahn-Teller ordered state[6] is realized below $T_{\rm JT} \approx 750\,$K, and an A-type antiferromagnetic (AFM) ordering of the Mn moments develops below $T_{\rm N}^{\rm Mn} \approx 140\,$K. This type of ordering is characterized by a ferromagnetic alignment of the magnetic moments within the ab planes, and an antiferromagnetic one along the c axis[7,8,9]. A Dzyaloshinski-Moriya (DM) type interaction $J_{\rm DM}$ causes a canting of the spins towards the c direction resulting in a weak ferromagnetic moment ($M_{\rm WF}$). This A-type AFM ordering remains for $R =$ Pr,…,Eu, but the Néel temperature is successively suppressed. There are three main exchange couplings between the Mn moments: the ferromagnetic nearest-neighbor (NN) coupling ($J_\parallel^{\rm FM}$) within the ab plane, the next-nearest neighbor (NNN) antiferromagnetic exchange interaction ($J_\parallel^{\rm AFM}$) within the ab plane, and the antiferromagnetic NN interaction $J_\perp^{\rm AFM}$ along the c direction. A larger distortion, i.e. a decreasing Mn-O-Mn bond angle, suppresses $J_\parallel^{\rm FM}$, whereas $J_\parallel^{\rm AFM}$ hardly changes[10,11,12]. The increasing frustration between $J_\parallel^{\rm FM}$ and $J_\parallel^{\rm AFM}$ destabilizes the A-type AFM ordering and finally leads to complex ordering phenomena for $R =$ Gd, Tb, and Dy[1,2,13,14,15,16,17,18,19,20]. For $R =$ Dy…Lu, RMnO$_3$ crystallizes either in a GdFeO$_3$-type or in a hexagonal structure depending on the growth technique, while for $R =$ Er, …, Lu usually the hexagonal structure is realized[21,22].

The presentation of our results in the subsequent sections is organized as follows. After a description of the experimental setup we first concentrate on the zero-field data obtained on NdMnO$_3$. Then we discuss the influence of a magnetic field applied either along the c axis or within the ab plane of NdMnO$_3$. In the last subsection our results obtained on TbMnO$_3$ will be analyzed.

II. RESULTS AND DISCUSSION

A. Experimental

The NdMnO$_3$ single crystal used in this study is a cuboid of dimensions $1.65 \times 1.85 \times 1.2\,\mathrm{mm}^3$ along the a, b, and c direction, respectively. It was cut from a larger crystal grown by floating-zone melting[23]. Magnetization and specific heat data of the same crystal are reported in Ref. 24. The measurements on TbMnO$_3$ have been performed on different small single crystals which were cut from a larger crystal grown by floating-zone melting in an image furnace[14]. The thermal conductivity was measured by a standard steady-state technique using a differential Chromel-Au+0.07%Fe-thermocouple[25]. For NdMnO$_3$, we studied κ_b with a heat current along the b axis in magnetic fields applied either along a, b, or c. All these measurements were performed with one set of heat contacts using either a 140 kOe longitudinal-field or a 80 kOe transverse-field cryostat. For TbMnO$_3$, we present measurements of κ_a, i.e. with a heat current along the a axis. Here, we used different configurations in order to allow measurements up to 140 kOe for all three field directions. Unfortunately, the TbMnO$_3$ crystal cracked when we increased the field above 110 kOe for $H \parallel c$. This problem also occurred on another TbMnO$_3$ crystal during our thermal-expansion measurements for the same field direction and we suspect that the crystals break because of strong internal torque effects[4]. The longitudinal thermal expansion coefficients α_i have been measured along all three crystal axes $i = a$, b, and c using different home-built high-resolution capacitance dilatometers[26,27,28]. For the field-dependent measurements, we concentrate on α_b of NdMnO$_3$ with $H \parallel c$ and $H \parallel b$ up to maximum fields of 140 kOe. Measurements with $H \parallel a$ were not possible due to large torque effects. For TbMnO$_3$, we only present zero-field data of α_i, since the field influence is discussed in detail in Ref. 4.

B. NdMnO$_3$ in Zero Magnetic Field

Figure 1a shows the uniaxial thermal expansion coefficients α_i $(i = a, b, c)$ of NdMnO$_3$. The Néel transition at $T_\mathrm{N}^\mathrm{Mn} \simeq 85\,\mathrm{K}$ causes large anomalies along all three crystallographic axes. The sign of the anomaly is positive for α_b and α_c, while it is negative for α_a. From Ehrenfest's relations it follows that the sign of the anomaly of α_i corresponds to the sign of the uniaxial pressure dependence of T_N. This means, for example, T_N^Mn would increase under uniaxial pressure applied either along the b or c axis. The different signs of the uniaxial pressure dependencies of T_N as well the suppression of T_N in the RMnO$_3$ series with increasing Mn-O-Mn bond angle can be essentially traced back to the frustration between the NN $J_\parallel^\mathrm{FM}$ and the NNN $J_\parallel^\mathrm{AFM}$ in the ab planes. For a more detailed discussion we refer to Refs. 3,4.

Figure 1b shows the zero-field thermal conductivity κ_b (left scale) together with the specific heat (right scale; data from Ref. 24). There is a λ-like peak in the specific heat at $T_\mathrm{N}^\mathrm{Mn} \simeq 85\,\mathrm{K}$ and at the same temperature κ_b has a sharp minimum. Above T_N, κ_b increases monotonically, which contradicts conventional phononic behavior. Below T_N, κ has a maximum at 25 K with a rather low value of 7 W/Km. Around 8 K the specific heat shows a Schottky peak, which arises from a splitting of the $4f$ ground-state doublet of the Nd^{3+} ions[24]. In general, a two-level Schottky peak is described by

$$C_\mathrm{sch} = k_B \cdot \frac{\Delta^2}{T^2} \cdot \frac{\tau_1 \tau_2 \exp(-\Delta/T)}{(\tau_1 + \tau_2 \exp(-\Delta/T))^2}, \qquad (1)$$

where τ_1 and τ_2 are the degeneracies of the involved levels and Δ the energy splitting. For NdMnO$_3$ we obtain $\Delta \simeq 21\,\mathrm{K}$ and $\tau_1 = \tau_2 = 1$. The $^4I_{9/2}$ ground-state multiplet of a free Nd^{3+} ion is ten-fold degenerate, but splits to five doublets in the orthorhombic crystal field (CF). To our knowledge, no neutron scattering investigations of the CF splitting of NdMnO$_3$ are available. However, in the related compounds NdAO$_3$ with $A =$Ni, Fe, and Ga a splitting of the order of 200 K between the ground-state doublet and the first excited doublet has been measured[29,30,31,32]. Since a similar CF splitting is expected for NdMnO$_3$, the observed Schottky anomaly cannot arise from a thermal population of the first excited doublet. Instead it has to be attributed to a zero-field splitting of the Nd^{3+} ground-state doublet, which arises from the exchange interaction between the canted Mn moments and the Nd moments[24]. A Schottky peak can also occur in α_i and its magnitude and sign are given by the uniaxial pressure dependence of the energy gap[4,33]. In NdMnO$_3$, an obvious Schottky contribution is only present for α_b, which will be analyzed in detail below.

In an insulator the heat is transported by phonons. This can be described by $\kappa \propto C v_\mathrm{s} \ell$, where C is the specific heat, v_s the sound velocity, and ℓ the mean free path of the phonons. At low temperatures ℓ is determined by boundary scattering, and κ follows the T^3 dependence of

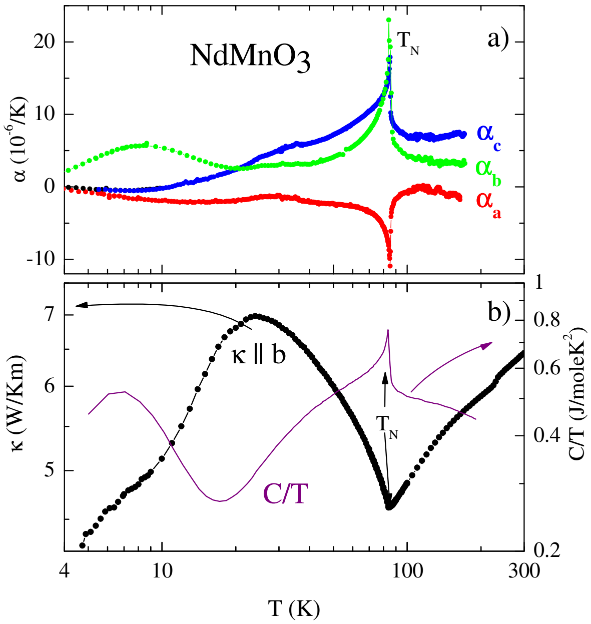

FIG. 1: (Color online) a) Thermal expansion of $NdMnO_3$ along all three crystallographic axes. b) Thermal conductivity measured with a heat current along the b axis (left scale) and specific heat (right scale; data from Ref. 24) of $NdMnO_3$.

the specific heat. At intermediate temperatures κ traverses a maximum with a height strongly determined by scattering of phonons by defects. At high temperatures C approaches a constant, and κ roughly follows a $1/T$ dependence due to Umklapp scattering.

Figure 2a compares the zero-field thermal conductivity of $NdMnO_3$ and $NdGaO_3$[34]. In $NdGaO_3$, the expected temperature dependence of conventional phononic thermal conductivity is observed, and in the whole temperature range κ is significantly larger than κ of $NdMnO_3$. This difference shows that additional scattering mechanisms are acting in $NdMnO_3$. For a quantitative analysis we use an extended Debye model[35], which yields

$$\kappa(T)=\frac{k_B^4T^3}{2\pi^2\hbar^3v_s}\int_0^{\Theta_D/T}\tau\left(x,T\right)\frac{x^4e^x}{\left(e^x-1\right)^2}dx. \qquad (2)$$

Here, Θ_D is the Debye temperature, v_s the sound velocity, ω the phonon frequency, $x=\hbar\omega/k_BT$, and $\tau\left(x,T\right)$ the phonon relaxation time. The scattering rates of different scattering mechanisms, which are independent of each other, sum up to a total scattering rate

$$\tau^{-1}(x,T)=\frac{v_s}{L}+D\omega^2+P\omega^4+UT\omega^3\exp\left(\frac{\Theta_D}{uT}\right). \qquad (3)$$

The four terms on the right-hand side refer to the scattering rates on boundaries, on planar defects, on point defects, and to phonon-phonon Umklapp scattering, respectively. The mean free path cannot become smaller than the lattice spacing giving a lower limit for κ. This is taken into account in equation (3) by a minimum mean free path $\ell_{\min}$ and replacing $\tau(x,T)$ by $\max\{\tau_\Sigma(x,T),\ell_{\min}/v_s\}$ (Ref. 36). Theoretical investigations of the scattering of phonons by magnetic excitations yield an additional scattering rate[37,38]

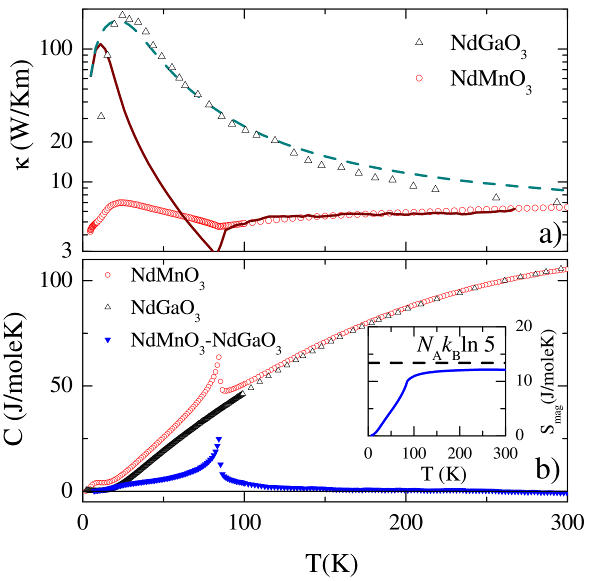

FIG. 2: (Color online) a) Zero-field thermal conductivity of $NdMnO_3$ (○) and $NdGaO_3$ (△) on a logarithmic κ scale. The lines are calculated within the Debye model using the parameters $\Theta_D = 600$ K, $v_s = 6000$ m/s, $P = 3.9\cdot10^{-43}\,\mathrm{s}^3$, $U = 6\cdot10^{-31}$ s/K, $u = 5.6$, and $l_{\min} = 9$ Å (see text). For the solid and dashed lines magnetic scattering has been included ($\epsilon = 4.5\cdot10^{-41}\,\mathrm{m}^3\mathrm{s}^3/\mathrm{KJ}$) and excluded ($\epsilon = 0$), respectively. b) Specific heat of $NdMnO_3$ (○, Ref. 24) and of $NdGaO_3$ (△, Ref. 34) as a reference compound. The magnetic contribution $C_m(T)$ (▼) due to Mn spin excitations is estimated by the difference of both curves. Inset: Magnetic entropy $S_m = \int C_m(T)/T\,dT$ (solid line) and expected $S_m = \mathrm{N_A}k_\mathrm{B}\ln(2S+1)\simeq 13.4$ J/molK (dashed) for the $S=2$ spins of Mn^{3+}.

$$\tau_m^{-1}=\epsilon T^2C_m(T)\omega^4, \qquad (4)$$

where ϵ describes the scattering strength, and C_m is the magnetic contribution to the specific heat. Note, that fluctuations may cause a sizeable C_m also above T_N.

In order to determine C_m the other contributions to C have to be subtracted. In $NdMnO_3$ this background contribution C_{bg} arises from acoustic and optical phonons as well as the Schottky specific heat of the $4f$ CF excitations of Nd^{3+}. Since a calculation of C_{bg} with the required precision is not possible, we use $NdGaO_3$ as a reference compound. Due to the structural similarity[39,40], the phonon spectrum and the CF splitting are presumably very similar in $NdGaO_3$ and $NdMnO_3$, apart from the additional splitting of the CF doublets of $NdMnO_3$. Figure 2b shows the specific heat of $NdMnO_3$[24] and $NdGaO_3$[34]. At high temperatures the curves are indeed nearly identical. We estimate

$$C_m(T) = C_{\mathrm{NdMnO_3}}(T) - C_{\mathrm{NdGaO_3}}(T) - C_{\mathrm{sch}}^{\Delta_0}(T). \quad (5)$$

The last term describes the Schottky contribution due to the splitting of the ground-state doublet and is calculated by equation (1) with $\Delta_0 = 21\,\mathrm{K}$ and $\tau_1 = \tau_2 = 1$. Note that the splittings of the excited doublets do not need to be considered, since their population sets in at higher temperature, and and as long as the splittings are not too large they hardly change the specific heat. In Fig. 2b we display the resulting C_m, which exhibits the λ peak at T_N and then slowly decays for $T > T_\mathrm{N}$. As a test of our analysis, we also calculate the magnetic entropy

$$S_m(T) = \int_0^T \frac{C_m}{T}dT. \quad (6)$$

As shown in the Inset of Fig. 2b, the experimental $S_m(T)$ approaches the expected $N_\mathrm{A} k_\mathrm{B} \ln(2S+1) \simeq 13.4\,\mathrm{J/moleK}$ of the Mn moments, where N_A and k_B denote Avogadro's number and Boltzmann's constant, respectively.

The dashed line of Fig. 2a shows the thermal conductivity calculated for $\mathrm{NdGaO_3}$ with the parameters given in the figure caption. The Debye temperature and the sound velocity have been estimated from the measured specific heat[24] and the other parameters have been adapted to fit the data. The calculated curve reproduces the general behavior of κ well. In order to describe the thermal conductivity of $\mathrm{NdMnO_3}$ the additional magnetic scattering rate τ_m^{-1} is switched on by adjusting the parameter ϵ, while keeping all the other parameters fixed. This calculation (solid line) describes the temperature dependence of κ above T_N very well. However, the calculation overestimates the minimum at T_N, and it shows a pronounced low-temperature maximum which is not present in the data. In principle, the latter difference could arise entirely from different point defect scattering in $\mathrm{NdMnO_3}$ and $\mathrm{NdGaO_3}$. However, our magnetic-field dependent measurements will show that this difference arises to a large extent from an additional phonon scattering on the CF levels.

C. NdMnO$_3$ in a Magnetic Field $H \parallel c$

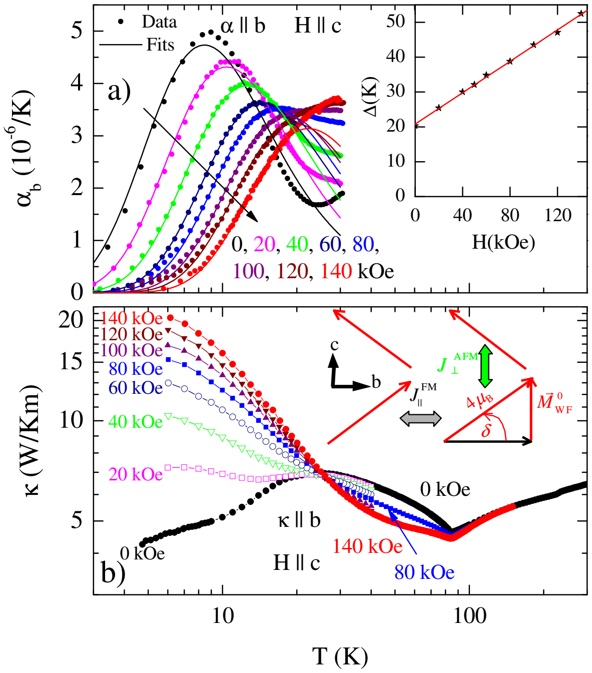

FIG. 3: (Color online) a) Thermal expansion α_b (symbols) of $\mathrm{NdMnO_3}$ for various magnetic fields $H \parallel c$ together with Schottky fits (solid lines). The arrow indicates the evolution of the Schottky peak with increasing field. Note the logarithmic temperature scale. Inset: Energy splitting Δ (symbols) of the $4f$ ground-state doublet of Nd^3 as a function of magnetic field. The line is a linear fit of $\Delta(H)$. b) Thermal conductivity of $\mathrm{NdMnO_3}$ for various $H \parallel c$ as a function of temperature on double-logarithmic scales. Inset: Sketch of the canting of the Mn spins along c (see text).

The low-temperature Schottky contribution to the thermal expansion of $\mathrm{NdMnO_3}$ is most pronounced for α_b; see Fig. 1. For a two-level system this contribution follows from a Grüneisen scaling between α and the specific heat[33], and for two singlets it gives

$$\alpha_{\mathrm{sch},i} = \frac{k_B}{V_{\mathrm{uc}}} \frac{\partial \ln(\Delta)}{\partial p_i} \left(\frac{\Delta}{T}\right)^2 \frac{e^{-\Delta/T}}{(1+e^{-\Delta/T})^2}\,. \quad (7)$$

Here, V_{uc} is volume per formula unit. The magnitude and the shape of $\alpha_{\mathrm{sch},i}(T)$ are entirely determined by the energy gap Δ and its uniaxial pressure dependence $\frac{\partial \ln(\Delta)}{\partial p_i}$. We conclude that $\frac{\partial \ln(\Delta)}{\partial p_i}$ is rather small for uniaxial pressure applied along a or c, since the Schottky contributions of α_a and α_c are so small that they are almost entirely masked by the respective phononic contributions. In contrast, α_b is clearly dominated by the Schottky contribution $\alpha_{\mathrm{sch},b}$ up to $\approx 20\,\mathrm{K}$. Thus, α_b allows for a detailed analysis of the magnetic-field dependence of the splitting of the Nd^{3+} ground-state doublet. Figure 3a shows α_b in magnetic fields up to 140 kOe applied along the c direction. With increasing field, the Schottky peak shifts monotonically to higher temperatures. The solid lines in Fig. 3a are fits via equation (7), which very well reproduce the experimental data and allow to derive the energy gap as a function of magnetic field. As shown in Fig. 3b we find a linear increase $\Delta(H) = 21\,\mathrm{K} + 2.25 \cdot 10^{-4}\,\mathrm{K/Oe} \cdot H$. The zero-field value nicely agrees with that obtained from the specific heat[24]. The field dependence of Δ can be understood as follows. In zero field, Δ_0 solely arises from the Nd-Mn exchange, which is proportional to the zero-field M_{WF}^0. A field applied along c increases Δ, on the one hand, due to the additional Zeeman splitting of the Nd^{3+} ground-state doublet. One the other hand, the canting of the Mn moments also increases with field, yielding an additional increase of the Nd-Mn exchange. Thus, for $H \parallel c$ we obtain

$$\Delta(H) = \frac{\tilde{a}}{k_{\rm B}}(M_{\rm WF}^0 + \chi_{\rm Mn} H) + \frac{g_{\rm Nd}\mu_{\rm B}}{k_{\rm B}} H\,. \tag{8}$$

Here, $\tilde{a}$ is the proportionality constant between $M_{\rm WF}$ and the Nd-Mn exchange, $\chi_{\rm Mn}$ the field-dependence of $M_{\rm WF}$, and $g_{\rm Nd}$ the g factor of the Nd^{3+} ground-state doublet.

For LaMnO$_3$ and PrMnO$_3$, values of $M_{\rm WF}^0 \simeq 0.1\mu_{\rm B}$ due to the DM interaction are reported[24,41]. A similar DM interaction can be expected for NdMnO$_3$, but due to the Nd-Mn exchange interaction additional energy can be gained from an enhanced splitting of the Nd^{3+} ground-state doublet by increasing the canting of the Mn spins. In order to estimate this effect we calculate the single-site energy of a Mn^{3+} ion as a function of the canting angle δ; see Fig. 3d. In a first step, we consider the zero-field case of PrMnO$_3$, where only $J_\perp^{\rm AFM}$, $J_{\rm DM}$, and the single-ion anisotropy D of Mn^{3+} have to be considered. Based on the Hamiltonian of Ref. 11 we obtain

$$E_0^{\rm Pr}(\delta) = -4J_\perp^{\rm AFM} S^2 \cos(2\delta) - 2J_{\rm DM}\sin\delta - D[S\cos\delta]^2 \tag{9}$$

where $S = 2$ is the Mn spin. Using $J_\perp^{\rm AFM}$= 7 K and $D = 0.9$ K from Ref. 42 and $\delta_0 = 1.4^\circ$ from $M_{\rm WF}^0 = 4\mu_{\rm B}\sin\delta_0 = 0.1\mu_{\rm B}$[24], we obtain $J_{\rm DM} = 5.7$ K from the minimization condition $\partial E/\partial\delta = 0$ at $\delta_0 = 1.4^\circ$. In the next step we include the additional energy gain in the Nd^{3+} ground-state doublet, which is given by $\Delta(H)/2$ from equation (8), and the potential energy of the Mn moment in a finite field $H \parallel c$. It is reasonable to assume that $J_\perp^{\rm AFM}$, $J_{\rm DM}$, and D do not change from PrMnO$_3$ to NdMnO$_3$ (see also Refs. 11,12,42). Thus, we keep these parameters fixed and obtain

$$E^{\rm Nd}(\delta, H) = E_0^{\rm Pr}(\delta) - \frac{\Delta(H)}{2} - \frac{M_{\rm WF}(\delta)H}{k_{\rm B}}\,. \tag{10}$$

The determination of the remaining parameters is straightforward. First $\partial E(\delta, H = 0)/\partial\delta = 0$ is solved for $H = 0$ under the additional condition that the zero-field value $\Delta_0 = 21$ K is reproduced. This yields $M_{\rm WF}^0 = 0.65\,\mu_{\rm B}$, $\delta_0 = 9.4^\circ$, and $\tilde{a} = 470$ kOe. Then $\chi_{\rm Mn}$ and $g_{\rm Nd}$ follow from a minimization of equation (10) for finite fields under the condition that the observed field dependence $\partial\Delta/\partial H = 2.25 \cdot 10^{-4}$ K/Oe is fulfilled. The resulting values are $g_{\rm Nd} = 2.2$ and $\chi_{\rm Mn} = 2.4 \cdot 10^{-6}\,\mu_{\rm B}$/Oe. Remarkably, the weak fm moment $M_{\rm WF}^0 = 0.65\,\mu_{\rm B}$ of NdMnO$_3$ is strongly enhanced compared to the values of $\simeq 0.1\,\mu_{\rm B}$ of PrMnO$_3$ or LaMnO$_3$. This enhancement should be clearly visible in a magnetic structure determination, which would be a good test of our analysis.

Figure 3b shows the thermal conductivity of NdMnO$_3$ up to $H = 140$ kOe applied along the c direction. At 5 K the thermal conductivity increases almost linearly with field up to $\kappa_b \simeq 20$ W/Km. This strong field dependence weakens with increasing temperature, and around 25 K the field dependence even changes sign and remains negative up $T \gtrsim T_{\rm N}$. Our data suggest that the low-temperature behavior of κ_b arises from resonant scattering of phonons between different levels of the $4f$ multiplet of Nd^{3+} which causes a suppression of the phonon heat transport in a certain temperature range. Such a suppression of κ by resonant scattering on $4f$ states is well-known from the literature[43]. The idea is that a phonon with an energy equal to the energy splitting of two $4f$ levels is first absorbed and then reemitted. Since the momenta of the incoming and reemitted phonons have arbitrary directions, an additional heat resistance is caused (for more details see e.g. Ref. 44). The comparison of the zero-field thermal expansion and the zero-field thermal conductivity data gives clear evidence that resonant scattering between the two levels of the split ground-state doublet is the cause for the strong suppression of κ at low temperatures. Since the splitting of the ground-state doublet increases with increasing field the scattering probability of the low-energy phonons systematically decreases resulting in a strong increase of the low-temperature thermal conductivity. In the temperature range above $\simeq 25$ K, the situation is more complex as will be discussed in the following subsection.

D. NdMnO$_3$ in Magnetic Fields $H \parallel a$ and $\parallel b$

Figure 4a shows the temperature-dependent thermal expansion α_b for magnetic fields $H \parallel b$ up to 80 kOe. Here, the behavior of the Schottky contribution is different to that observed for $H \parallel c$. For small fields ($H \leq$ 20kOe) almost no effect occurs while for higher fields the peak height continuously decreases until it disappears completely for $H \simeq 80$ kOe. The maximum of the peak weakly shifts to higher temperature when the field is increased from 0 to 60 kOe. This weak increase is a consequence of the perpendicular orientation of the external magnetic field with respect to the exchange field arising from $M_{\rm WF} \| c$. Thus, the total effective field is given by the vector sum of both contributions, which for small external fields only weakly increases. The decrease of the peak height and its disappearance at 80 kOe suggest that the pressure dependence of the energy gap also decreases with field and finally vanishes. Whether this is really the case is, however, not clear because around 100 kOe a spin-flop transition takes place for this field direction[24]. Thus, different energy scales have to be considered, which prevent a simple analysis of the pressure dependencies via a Grüneisen scaling[33]. As displayed in Fig. 4b, α_b for $H \geq 100$ kOe$\|b$ has another anomaly, which we attribute to the spin-flop transition. This anomaly strongly shifts towards higher temperatures with further increasing field, i.e. the phase with $M_{\rm WF} \| c$ becomes less stable towards lower temperatures.

Figure 5 shows κ for $H \parallel a$ and $\|b$, which is suppressed in the entire range $T \lesssim T_{\rm N}$ for both field directions. This behavior is in clear contrast to the strong low-

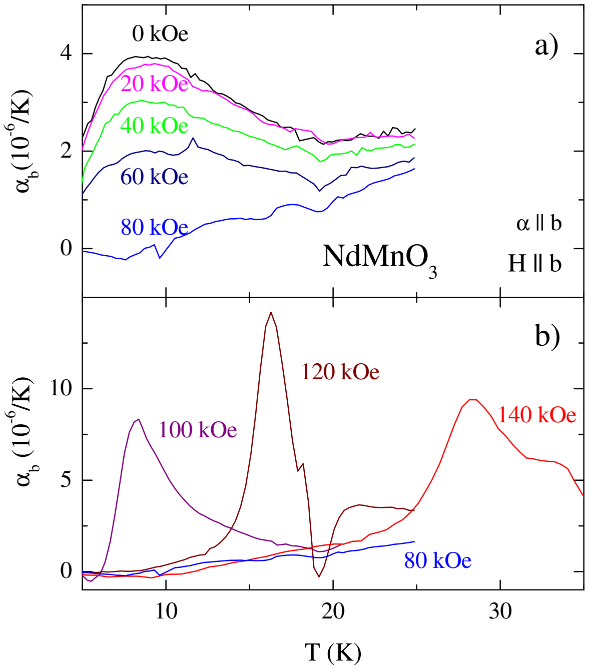

FIG. 4: (Color online) Thermal expansion α_b of NdMnO$_3$ with $H \parallel b$ up 80 kOe and above 100 kOe.

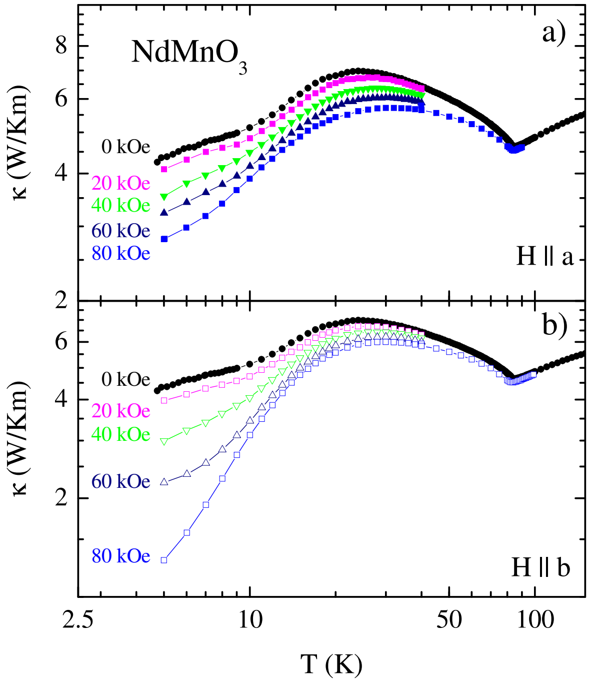

FIG. 5: (Color online) Thermal conductivity κ_b of NdMnO$_3$ in magnetic fields $H \parallel a$ and $H \parallel b$.

temperature increase of κ for $H \parallel c$, whereas the weak decrease of κ above about 30 K is rather similar for all three field directions. Thus we conclude that the field dependence of κ_b is determined by two different scattering mechanisms. Firstly, there is the resonant scattering within the split ground-state doublet. This scattering is strongly suppressed at low temperature for $H \parallel c$ because of the increasing splitting. As discussed above, the splitting increases much less for $H \parallel a$ and $H \parallel b$, since the effective field increases only weakly for $H \perp M_{\mathrm{WF}}$. Nevertheless, a low-temperature *increase* of κ_b should occur for $H \parallel a$ and $H \parallel b$ if this resonant scattering was the only field dependent scattering process. To explain the observed decrease of κ_b requires another scattering process which increases with magnetic field for all three field directions. This second process is only visible when the field dependence of the first resonant one is weak, i.e., for $H \parallel a$ and $H \parallel b$ in comparatively weak fields and for $H \parallel c$ at $T \gtrsim 25$ K. Since the field dependence of κ_a essentially vanishes slightly above T_{N} we suspect that this second field dependent scattering process is related to scattering of phonons by magnons, but the presence of higher-lying CF levels of Nd^{3+} could also play a role.

E. TbMnO$_3$

TbMnO$_3$ is the first compound of the RMnO$_3$ series in which ferroelectricity has been established over a large temperature and magnetic-field range. The phase diagram was first explored by polarization and magnetization data in Ref. 15 and recently it has been refined by thermal expansion measurements[4]. In zero field, the system transforms from a paramagnetic to an incommensurate antiferromagnetic phase (HTI) at $T_{\mathrm{N}} \simeq 41$ K. At $T_{\mathrm{FE}} \simeq 27$ K, a transition occurs into another incommensurate antiferromagnetic phase (LTI) with a different propagation vector. This phase is ferroelectric with a polarization along c. The phase boundaries at T_{N} and T_{FE} hardly depend on a magnetic field, but for $H \parallel a$ and $\parallel b$ a transition from the LTI phase to a commensurate antiferromagnetic phase (LTC) occurs below T_{FE}, which is accompanied by a polarization flop from $P \parallel c$ to $P \parallel a$. The main difference between $H \parallel a$ and $H \parallel b$ is the much larger hysteresis of the LTI-to-LTC transition for $H \parallel a$. A magnetic field along c causes a transition into a paraelectric canted AFM phase above $\simeq 7$ T.

Figure 6(a-c) shows the thermal conductivity of TbMnO$_3$ along the a direction. In zero field, κ_a has a broad minimum around 80 K and a weak maximum at T $\simeq$ 34 K with a relatively low absolute value $\kappa \approx 3$ W/Km. Figure 6d displays the thermal expansion of TbMnO$_3$ in zero field along the a, b, and c axes. The transitions at T_{N} and T_{FE} cause anomalies of α along all three crystallographic directions, which are discussed in detail in Ref. 4. In addition, for all three directions broad Schottky contributions of different signs are present around 80 K, which originate from the $4f$ states of Tb^{3+}. The $^7F_6$ state of the free Tb^{3+} ion splits into 13 singlets in an orthorhombic CF. To our knowledge, the $4f$ energy level scheme of Tb^{3+} in TbMnO$_3$ is not

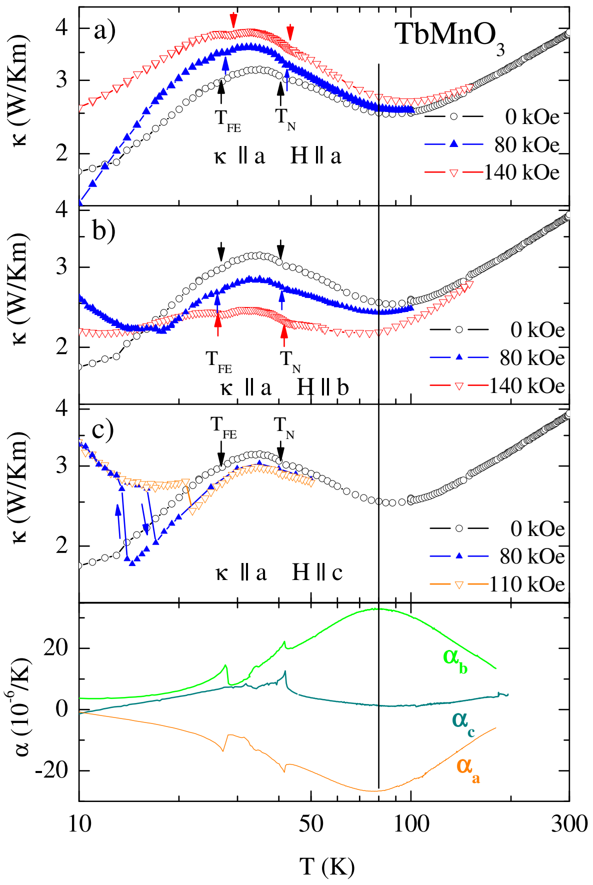

FIG. 6: (Color online) a-c): Thermal conductivity κ_a of $\mathrm{TbMnO_3}$ in magnetic fields along the different crystal axes. d) Thermal expansion α_i of $\mathrm{TbMnO_3}$ with $i = a$, b, and c. The vertical line is a guide for the eyes.

known[45] and we are not aware of any investigations of the crystal-field splitting of related TbAO$_3$ compounds. Thus, a detailed analysis of this Schottky contribution to α is not possible. As a rough estimate of the relevant energy scale a fit of the thermal expansion data by equation (7) yields an effective energy gap of $\approx 190\,\mathrm{K}$. The comparison of the thermal conductivity with the thermal expansion data shows that the extrema of α_i occur close to the minimum of κ. This correlation strongly suggests that the minimum of κ_a at $\approx 90\,\mathrm{K}$ is caused by resonant scattering of phonons between different CF levels of Tb^{3+}. Such an interpretation is further supported by the magnetic-field dependencies of κ_a. For $H \parallel b$ and $H \parallel c$, κ_a is suppressed over a broad temperature range, whereas it is enhanced for $H \parallel a$. These large field dependencies up to high temperatures are rather unusual, and clearly not related to the low-temperature ordering phenomena below 41 K. The influence of the various transitions below 41 K on κ_a is weak. We only observe small dips at the transition temperatures T_N and T_FE as indicated by the arrows in Fig. 6. The shape of the thermal conductivity curves remains essentially unchanged. We conclude that these ordering transitions play little role for κ_a, since the low κ_a is completely dominated by the scattering of phonons by the $4f$ CF levels of Tb^{3+}.

Below T_FE additional magnetic-field dependencies are observed. One can distinguish the measurements with $H \parallel a$ or b, where the LTI-to-LTC transition occurs, from those with $H \parallel c$, where the system turns into the paraelectric phase for sufficiently large fields. For the latter case, a sharp increase of κ_a is observed when the paraelectric phase is reached, see Fig. 6c. The pronounced hysteresis of the 80 kOe curve reflects the first-order nature of this transition. Apart from the different transition temperatures, the curves for 80 kOe and 110 kOe are almost identical. For $H = 80\,\mathrm{kOe} \parallel b$, κ_a increases at the LTI-to-LTC transition ($\approx$ 18 K; see Fig. 6b). Although this field dependence is of opposite sign compared to the high-temperature field dependence for $H \parallel b$, it is difficult to separate both effects, because the scattering by the CF levels of Tb^{3+} probably causes a magnetic-field dependence of κ down to the lowest temperature. Since the LTI-to-LTC transition is accompanied by a polarization flop from $P \parallel a$ to $P \parallel c$, one may suspect that the increase of κ_a is related to the formation of ferroelectric domains. We have, however, ruled out this possibility by measurements of the electrical polarization as well as of the thermal conductivity under application of large electrical fields (not shown). Although the domain formation could be clearly seen in the polarization measurements, no electric-field influence was detectable in κ. Thus, another explanation for the suppressed thermal conductivity in the LTI phase is needed. Probably, it is the incommensurability itself, which causes an additional thermal resistance, because the crystal symmetry is lowered in the LTI phase. Accordingly, one should expect a similar behavior for $H \parallel a$, but the broadening of the LTI-to-LTC transition due to its large hysteresis[4] and the superimposed high-temperature field dependence prevent a separation of the different effects at low temperatures. The incommensurability is also consistent with the jump of κ for $H \parallel c$, since the paraelectric phase is commensurate and therefore of higher symmetry.

III. CONCLUSIONS

We have studied the thermal expansion and thermal conductivity of $\mathrm{NdMnO_3}$ and $\mathrm{TbMnO_3}$ under application of large magnetic fields. The thermal conductivity of $\mathrm{NdMnO_3}$ is a very unusual. The Néel transition at $T_\mathrm{N} \simeq 85\,\mathrm{K}$ leads to a strong suppression of the phonon thermal conductivity over a large temperature range. Including a magnetic scattering rate proportional to the magnetic specific heat allows us to describe the thermal conductivity from T_N to room temperature. At low temperatures the thermal conductivity is further suppressed by another scattering mechanism. The $4f$ ground-state doublet of Nd^{3+} is split ($\Delta_0 \approx 21\,\mathrm{K}$) by an exchange interaction with the canted Mn moments. Our analysis suggests a significant enhancement of the Mn canting angle in $NdMnO_3$ compared to that in $PrMnO_3$ as a consequence of this Nd-Mn interaction. The splitting of the ground-state doublet thereby allows for resonant scattering of phonons which causes the additional suppression of κ in zero field. The analysis of the thermal expansion in magnetic fields up to 140 kOe reveals that $\Delta(H)$ strongly increases in magnetic fields $H \parallel c$. This increase of $\Delta(H)$ shifts the effectiveness of the resonant scattering processes towards higher temperature and causes a drastic increase of κ at low temperatures. For $H \parallel c$, with increasing temperature a gradual change occurs leading to a suppression of κ. A similar suppression is present for $H \parallel a$ and $H \parallel b$ in the entire low-temperature range. This requires the presence of a second field-dependent scattering mechanism, which may be related to scattering of phonons either by magnons or by higher-lying CF levels.

$TbMnO_3$ also exhibits a strongly suppressed thermal conductivity over the entire temperature range. The clear correlation of the temperature dependencies of κ and of the uniaxial thermal expansion coefficients α enables us to conclude that the dominant mechanism suppressing κ is resonant scattering of phonons by the $4f$ CF levels of Tb^{3+}. The interpretation of Ref. 5 that the low absolute values of the thermal conductivity of $TbMnO_3$ should be caused by the complex magnetic and electric ordering phenomena is ruled out by our data. In contrast, the complex transitions of $TbMnO_3$ only cause very weak anomalies in κ at T_N and T_{FE}. A somewhat larger influence is present at the transitions induced by finite magnetic fields. The LTI-to-LTC transition for $H \parallel a, b$ as well as the transition to the paraelectric phase for $H \parallel c$ cause an increase of the thermal conductivity. Probably, this increase of κ arises from the incommensurability of the LTI phase, which is transformed to a commensurate phase of higher symmetry for all three field directions. We also found that the ferroelectric domain structure has no measurable influence on the heat transport in $TbMnO_3$.

Acknowledgments

We acknowledge useful discussions with P. Hansmann, M. Haverkort, D. Khomskii, D. Senff, and A. Sologubenko. This work was supported by the Deutsche Forschungsgemeinschaft through SFB 608.

---

[1] T. Kimura, S. Ishihara, H. Shintani, T. Arima, K.T. Takahashi, K. Ishizaka, and Y. Tokura. Nature **426**, 55–58 (2003).

[2] J. Baier, D. Meier, K. Berggold, J. Hemberger, A. Balbashov, J.A. Mydosh, and T. Lorenz. Phys. Rev. B **73**, 100402(R) (2006).

[3] J. Baier, D. Meier, K. Berggold, J. Hemberger, A. Balbashov, J.A. Mydosh, and T. Lorenz. cond-mat/0605515 (2006).

[4] D. Meier, N. Aliouane, D.N. Argyriou, J.A. Mydosh, and T. Lorenz. cond-mat/0701487 (2007).

[5] J.S. Zhou and J.B. Goodenough. Phys. Rev. Lett. **96**, 247202 (2006).

[6] J. Rodríguez-Carvajal, M. Hennion, F. Moussa, A.H. Moudden, L. Pinsard, and A. Revcolevschi. Phys. Rev. B **57**, R3189 (1998).

[7] E.O. Wollan and W.C. Koehler. Phys. Rev. **100**, 545 (1955).

[8] J.B. Goodenough, A. Wold, R.J. Arnott, and N. Menyuk. Phys. Rev. **124**, 373 (1961).

[9] S. Ishihara, J. Inoue, and S. Maekawa. Phys. Rev. B **55**, 8280 (1997).

[10] R. Kajimoto, H. Mochizuki, H. Yoshizawa, H. Shintani, T. Kimura, and Y. Tokura. J. Phys. Soc. Japan **74**, 2430 (2005).

[11] F. Moussa, M. Hennion, J. Rodriguez-Carvajal, H. Moudden, L. Pinsard, and A. Revcolevschi. Phys. Rev. B **54**, 15149 (1996).

[12] K. Hirota, N. Kaneko, A. Nishizawa, and Y. Endoh. J. Phys. Soc. Japan **65**, 3736 (1996).

[13] T. Arima, T. Goto, Y. Yamasaki, S. Miyasaka, K. Ishii, M. Tsubota, T. Inami, Y. Murakami, and Y. Tokura. Phys. Rev. B **72**, 100102(R) (2005).

[14] N. Aliouane, D.N. Argyriou, J. Strempfer, I. Zegkinoglou, S. Landsgesell, and M.v. Zimmermann. Phys. Rev. B **73**, 020102(R) (2006).

[15] T. Kimura, G. Lawes, T. Goto, Y. Tokura, and A.P. Ramirez. Phys. Rev. B **71**, 224425 (2005).

[16] M. Kenzelmann, A.B. Harris, S. Jonas, C. Broholm, J. Schefer, S.B. Kim, C.L. Zhang, S.-W. Cheong, O.P. Vajk, and J.W. Lynn. Phys. Rev. Lett. **95**, 087206 (2005).

[17] T. Kimura, S. Ishihara, H. Shintani, T. Arima, K.T. Takahashi, K. Ishizaka, and Y. Tokura. Phys. Rev. B **68**, 060403(R) (2003).

[18] S. Quezel, F. Tcheou, J. Rossat-Mignoda, G. Quezel, and E. Roudaut. Physica B **86-88**, 916–918 (1977).

[19] J. Zukrowski, M. Wasniowska, Z. Tarnawski, J. Przewoznik, J. Chmist, A. Kozlowski, K. Krop, and M. Sawicki. Acta Physica Polonica B **34**, 1533–1535 (2003).

[20] T. Goto, Y. Yamasaki, H. Watanabe, T. Kimura, and Y. Tokura. Phys. Rev. B **72**, 220403(R) (2005).

[21] The manganites with $R=$ Er, …, Lu have been prepared in perovskite structure by high-pressure synthesis[46]. Here, an E-type antiferromagnetic ordering occurs below $T_N \approx 40\,K$.

[22] For the thermal conductivity in the hexagonal phase other mechanisms are dominant, e.g. rattler atoms[5,47].

[23] A.M. Kadomtseva, Yu.F. Popov, G.P. Vorobév, K.I. Kamilov, A.P. Pyatakov, V.Yu. Ivanov, A.A. Mukhin, and A.M. Balbashov. Sov. Phys. JETP Lett. **81**, 22–26 (2005).

[24] J. Hemberger, M. Brando, R. Wehn, V.Y. Ivanov, A.A. Mukhin, A.M. Balbashov, and A. Loidl. Phys. Rev. B **69**, 064418 (2004).

[25] K. Berggold, T. Lorenz, J. Baier, M. Kriener, D. Senff, H. Roth, A. Severing, H. Hartmann, A. Freimuth, S. Barilo, and F. Nakamura. Phys. Rev. B **73**, 104430 (2006).

[26] R. Pott and R. Schefzyk. J. Phys. E – Sci. Instrum. **16**, 444 (1983).

[27] T. Lorenz, U. Ammerahl, T. Auweiler, B. Büchner, A. Revcolevschi, and G. Dhalenne. Phys. Rev. B **55**, 5914 (1997).

[28] O. Heyer. *Diploma thesis*, University of Cologne (2005).

[29] W. Marti, M. Medarde, S. Rosenkranz, P. Fischer, A. Furrer, and C. Klemenz. Phys. Rev. B **52**, 4275 (1995).

[30] A. Podlesnyak, S. Rosenkranz, F. Fauth, W. Marti, A. Furrer, A. Mirmelstein, and H.J. Scheel. J. Phys. – Condens. Matter **5**, 8973 (1993).

[31] S. Rosenkranz, M. Medarde, F. Fauth, J. Mesot, M. Zolliker, A. Furrer, U. Staub, P. Lacorre, R. Osborn, R.S. Eccleston, and V. Trounov. Phys. Rev. B **60**, 14857 (1999).

[32] R. Przenioslo, I. Sosnowska, M. Loewenhaupt, and A. Taylor. J. Magn. Magn. Mat. **140**, 2151 (1995).

[33] T. Lorenz, S. Stark, O. Heyer, N. Hollmann, A. Vasiliev, and A. Oosawa and H. Tanaka. cond-mat/0609348 (2006).

[34] W. Schnelle, R. Fischer, and E. Gmelin. J. Phys. D – Applied Phys. **34**, 846 (2001).

[35] R. Bermann. *Thermal Conduction in Solids.* Clarendon Press Oxford (1976).

[36] K. Kordonis, A.V. Sologubenko, T. Lorenz, S. W. Cheong, and A. Freimuth. Phys. Rev. Lett. **97**, 115901 (2006).

[37] K. Kawasaki. Prog. Theor. Phys. **29**, 801 (1963).

[38] H. Stern. J. Phys. Chem. Solids **26**, 153 (1965).

[39] W. Marti, P. Fischer, J. Schefer, and F. Kubel. Z. f. Krist. **211**, 891 (1996).

[40] T. Mori, N. Kamegashira, K. Aoki, T. Shishido, and T. Fukuda. Materials Letters **54**, 238 (2002).

[41] M. Paraskevopoulos, F. Mayr, J. Hemberger, A. Loidl, R. Heichele, D. Maurer, V. Muller, A.A. Mukhin, and A.M. Balbashov. J. Phys. – Condens. Matter **12**, 3993 (2000).

[42] R. Kajimoto, H. Yoshizawa, H. Shintani, T. Kimura, and Y. Tokura. Phys. Rev. B **70**, 012401 (2004).

[43] P.V.E. Mcclintock, I.P. Morton, R. Orbach, and H.M. Rosenberg. Proc. Roy. Soc. Lond. **A298**, 359 (1967).

[44] M. Hofmann, T. Lorenz, G.S. Uhrig, H. Kierspel, O. Zabara, A. Freimuth, H. Kageyama, and Y. Ueda. Phys. Rev. Lett. **87**, 047202 (2001).

[45] In Ref. 42 a peak at 4 meV observed by neutron scattering was attributed to a CF excitation, but these measurements were restricted to $E < 10\,\mathrm{meV}$.

[46] J.-S Zhou, J.B. Goodenough, J.M. Gallardo-Amores, E. Morán, M.A. Alario-Franco, and R. Caudillo. Phys. Rev. B **74**, 014422 (2006).

[47] P.A. Sharma, J.S. Ahn, N. Hur, S. Park, S.B. Kim, S. Lee, J.G. Park, S. Guha, and S.W. Cheong. Phys. Rev. Lett. **93**, 177202 (2004).